Intra-Day Direct Normal Irradiance Forecasting Under Clear Sky Conditions Using ANFIS

Rémi Chauvin, Julien Nou, Stéphane Thil, Stéphane Grieu

Intra-Day Direct Normal Irradiance Forecasting Under Clear Sky Conditions Using ANFIS

Rémi Chauvin * **Julien Nou** * **Stéphane Thil** *,** **Stéphane Grieu** *,**

* *Laboratoire PROMES-CNRS (UPR 8521), Tecnosud, Rambla de la thermodynamique, 66100 Perpignan, France*
** *University of Perpignan Via Domitia, 52 Avenue Paul Alduy, 66860 Perpignan, France*

Tel.: +334-6868-2222; e-mail: firstname.lastname@promes.cnrs.fr

Abstract: This paper deals with an intra-day Direct Normal Irradiance (DNI) forecasting methodology under clear sky conditions, for time horizon varying up to 5 h. The goal is to evaluate the variability and the needs of forecasting models under such conditions. It is a part of a project which aims to forecast the DNI under various sky conditions at short term horizon and high spatial resolution. A quick review of the clear sky DNI modeling is firstly performed. Then, the database selection and filtering process is described. Finally, the forecasting approaches are presented and compared to persistent models used as references. The most efficient model presented here is based on adaptive network-based fuzzy inference systems and the optimal configuration achieves very good forecasting results and validates the proposed methodology.

Keywords: Adaptive Network-based Fuzzy Inference Systems, Direct Normal Irradiance, Clear Sky Models, Time Series Forecasting.

1. INTRODUCTION

In a context of sustainable development, clean energy systems are strongly promoted in the European energy mix. Among the various solar energy systems, the Concentrating Solar Power (CSP) systems will play a key role in the future [Agency, 2010]. At this stage, the main drawback of this technology continues to be its cost. To overcome it, the European research project CSPIMP (Concentrated Solar Power plant IMProvement) has been recently initiated. Its main target is to achieve a better competitiveness of the CSP plants thanks to the development of new tools improving steam turbine start up cycles, maintenance activities and plant control.

One challenge of the project is to better forecast the sun's resource. Indeed, it is widely acknowledged by producers and grid operators that solar energy variability strongly influences the CSP systems output. Therefore, Direct Normal Irradiance (DNI) forecasting would help them to efficiently schedule and manage the electricity production according to the grid needs. Different solar irradiance forecast methodologies have already been developed for various time horizons [Diagne et al., 2013]. Changes in the DNI are mainly affected by clouds motion, which can be detected using sky camera or satellite imagery [Mefti et al., 2008] [Zaher, 2012] [Chow et al., 2011] [Marquez and Coimbra, 2013] [Cazorla et al., 2008]. When there is no clouds, however, the atmospheric turbidity, mainly attributable to the Aerosol Optical Depth (AOD), is known to be the driving factor [Gueymard, 2012b]. As a consequence, it has been decided to split the DNI forecasting in two different blocks: the cloud cover forecasting and the DNI forecasting under clear sky conditions. It is expected that this methodology would lead to more accurate forecasts than a global model. In this paper, only the clear sky DNI forecasting at different short-time horizons is studied.

First, a quick review of the atmospheric turbidity coefficients is introduced. It especially explains the choice of the model used according to our forecasting needs. The second part briefly describes the database used for our models as well as the multi-resolution analysis performed to extract the clear sky data. The next part focuses on the different models developed, based on the generated historical data of atmospheric turbidity. Then models are compared and discussed. The paper ends with a conclusion and outlook on further work.

2. CONSIDERATIONS ABOUT ATMOSPHERIC TURBIDITY

Under clear sky conditions, the broadband DNI (I_{CS}) is equal to the solar constant ($I_0 = 1367\,\mathrm{W/m^2}$) weighted by the sun-earth distance correction factor (r) and the atmospheric transmittance (T) resulting from both scattering and absorption of the sunlight. The equation can be expressed as follows:

$$I_{CS} = r I_0 T \tag{1}$$

The knowledge of the clear sky atmospheric transmittance is thus required to assess the amount of direct solar energy reaching the ground. This attenuation factor T is corre-

lated to the band transmittances of Rayleigh scattering (T_{Ra}), uniformly mixed gases absorption (T_g), ozone absorption (T_{O_3}), nitrogen dioxide absorption (T_{NO_2}), water vapor absorption (T_w) and aerosol absorption (T_{AOD}) as follows [Gueymard, 2008]:

$$T = T_{Ra}T_gT_{O_3}T_{NO_2}T_wT_{AOD} \quad (2)$$

All these transmittances are function of the sunlight optical path length (m) through the atmosphere, also called air mass. Information regarding to these atmospheric attenuation coefficients can be obtained using radiation transfer models based on site pressure, ozone amount, total nitrogen dioxide amount, precipitable water and Ångström turbidity coefficients as inputs parameters.

Among all clear-sky broadband radiation models of the literature, REST2 [Gueymard, 2008] has proven to predict DNI with unsurpassed accuracy [Gueymard and Myers, 2008] [Gueymard, 2012a]. However, the model requires AOD data which happens to be highly variable in both space and time, as well as difficult to measure [Gueymard, 2012b]. As a consequence, this model is not well adapted for on-site real-time clear sky DNI forecasting.

On the other hand, simpler models, based on a turbidity coefficient like the well-known Linke turbidity coefficient [Linke, 1922], have been developed. Although they have a lower accuracy than radiation transfer models, they have been widely used by the scientific community because they only derive from broadband beam radiation measurement networks and can thus be easily implemented.

The Linke turbidity coefficient represents the number of clean dry atmospheres leading to the observed attenuation of solar radiation. For instance, the average Linke turbidity is close to 3 in most parts of Europe whereas it can grow up to 6 or 7 in polluted cities. Although this coefficient is easy to calculate, one of its main drawbacks is its strong dependency on air mass [Kasten, 1988] [Grenier et al., 1994] [Kasten and Young, 1989]. That is why, in 2002, Ineichen and Perez proposed a new formulation of the Linke turbidity coefficient in order to limit this turbidity dependence upon solar geometry [Ineichen and Perez, 2002]. They obtained a new empirical formulation of the broadband atmospheric transmittance for the normal beam clear sky radiation:

$$T = f(m, T_{LI}) = b.\exp\left[-0.09 \cdot m(T_{LI} - 1)\right] \quad (3)$$

It can be noticed that the transmittance presented in (2) includes the effects of both scattering and absorption phenomena. This equation matches with the Linke turbidity coefficient at air mass 2 ($f(2, T_{LK}) = f(2, T_{LI})$) and is also corrected by a multiplicative coefficient b taking into account the altitude (alt) of the considered site:

$$b = 0.664 + \frac{0.163}{\exp\left(-alt/8000\right)} \quad (4)$$

From (1) and (3), Ineichein obtains a new turbidity coefficient that proves to have a much better stability than the previous one:

$$T_{LI}(t) = 1 + \left[\frac{11.1}{m(t)} \cdot \ln\left(\frac{b \cdot r(t) \cdot I_0}{I_{CS}(t)}\right)\right] \quad (5)$$

Because this coefficient can be easily derived from broadband beam radiation measurements, it has been selected as a starting point for the development of our intra-day clear sky DNI forecasting model.

3. DATA PRE-PROCESSING

The database used to develop and validate the different proposed DNI forecasting models is derived from data collected at the National Renewable Energy Laboratory, located in Golden, Colorado, USA. Data are freely available at *http://midcdmz.nrel.gov/apps* where an exhaustive set of meteorological parameters and irradiances are collected and stored since July 1981. In our study, only data ranging from 2002 to 2013 have been considered. Using (5), the following data have been collected:

- Timestamp
- Air mass (m)
- Extraterrestrial irradiance (I_0)
- Direct Normal Irradiance (I)

Different families of wavelets may be chosen for analyzing sequences of data points. The main criteria are (a) the time and frequency localizations, quantified by the speed of convergence to 0 of these functions when time and frequency goes to infinity, (b) the symmetry, (c) the number of vanishing moments of the mother wavelet and (d) the regularity, useful for getting nice features, like smoothness of the reconstructed signal. The most commonly used wavelets are the orthogonal ones (Daubechies, Symlet or Coiflet wavelets). Because the Daubechies wavelets [Daubechies, 1992] have the highest number of vanishing moments, this family has been chosen for carrying out the wavelet-based multi-resolution analysis of the considered data sequences.

The impact of both the decomposition level and the wavelet order on the algorithm performance has been studied [Nou et al., 2013] and the optimal configuration chosen is a decomposition of level 3, using 4^{th}-order Daubechies wavelets. **pas clair à partir de là, D_3 non défini, etc.** Clear sky data were selected by thresholding the detail D_3 and removing the low I values from the database. The clear sky irradiance threshold has been set to $150\,\mathrm{W/m^2}$ because this value refers to the typical minimum solar irradiance usable for CSP plant. With this selection, only full clear sky days were selected. Indeed, full days allow keeping the transient behavior of the turbidity, which is essential in our forecasting model. Finally, a temporal smoothing, using a moving average of 40 minutes, was applied on these selected days in order to remove the last outliers.

From these selected days, the turbidity is computed using (5). The final database specifications are reported in Table 1.

Table 1. Database specifications.

Description	Value
Latitude	39.74 N
Longitude	105.18 W
Altitude	1829 m
Number of selected clear sky days	156
Range	2002–2013
Yearly mean turbidity	2.37
Distribution [Spring Summer Autumn Winter]	[22 45 53 36]

4. MODELS

Different models have been developed and compared for forecast horizons varying from 30 minutes to 5 hours. The first category of models is based on the daily, monthly and yearly mean turbidity values. This approach allows to evaluate the gain of accuracy obtained from a yearly atmospheric turbidity coefficient to a daily one. The second category consists in two simple persistent models. They are used to validate the last category of models which is based on neuro-fuzzy systems. The different approaches are presented Figure 1.

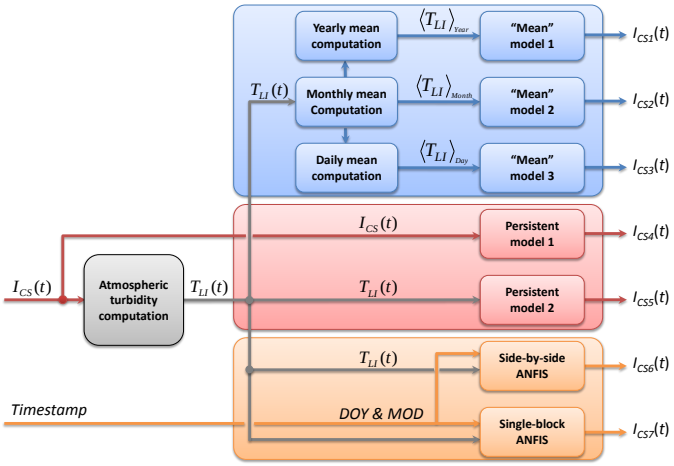

Fig. 1. Overview of the developed models.

4.1 Mean turbidity-based models

It is known that atmospheric turbidity has seasonal trends. The turbidity is higher in summer than in winter, because of a higher concentration in aerosol. Consequently, we decided to estimate the error between the clear sky irradiance measured and the irradiance calculated using the yearly, monthly and daily mean turbidity. These errors will also be used as reference for the next models. However, it is important to notice that these models cannot be considered as forecasting models because they only depend on the mean turbidity value. Thus, the error does not vary with time horizon. Figure 2 summarizes the mean values of turbidity through the year using the collected database. As expected, a seasonal trend of the turbidity can be observed with a peak during summer time. The yearly mean turbidity is averaged from the monthly mean turbidity whereas the daily mean turbidity comes from a linear interpolation of the monthly mean turbidity. According to (1) and (5), the expected clear sky irradiance of the collected days can be calculated as follows:

$$I_{CS_k}(t) = r(t) \cdot I_0 \cdot f\left(m(t), \langle T_{LI} \rangle_k\right) \tag{6}$$

where $k = \{\text{Year}, \text{Month}, \text{Day}\}$.

4.2 Persistent models

Two persistent models have been also tested on the database. The first one considers the DNI constant between the present and the forecast horizon whereas the second one considers the turbidity as a constant during the same elapsed time. Although the first persistent model is not expected to give good results, we compute it in order to highlight the relevancy of the turbidity coefficient use. Irradiance for both models can be expressed as follows:

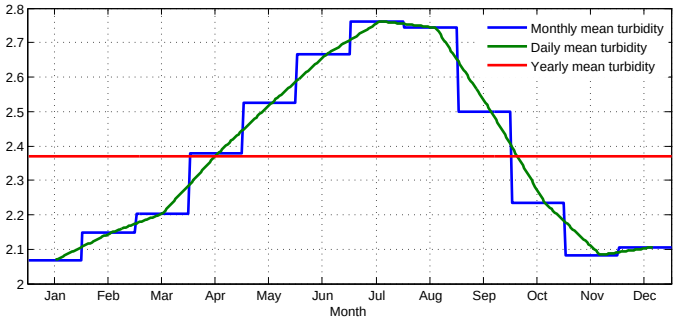

Fig. 2. Yearly, monthly and daily mean turbidity values

$$I_{CS_{p1}}(t + \Delta t) = I_{CS}(t) \tag{7}$$

$$I_{CS_{p2}}(t + \Delta t) = r(t + \Delta t) \cdot I_0 \cdot f\left(m(t + \Delta t), T_{LI}(t)\right) \tag{8}$$

4.3 ANFIS models

The new approach developed in this paper is based on ANFIS (Adaptive Network-Based Fuzzy Inference Systems) techniques. In the field of artificial intelligence, neural networks and fuzzy logic can be combined in neuro-fuzzy systems in order to achieve both properties of readability and learning ability. Neuro-fuzzy systems synergizes the two techniques by combining the human-like reasoning style of fuzzy systems (through the use of fuzzy sets and a linguistic model consisting of a set of if-then fuzzy rules) with the learning and connectionist structure of artificial neural networks [Lin and Lee, 1996] [Abraham, 2005].

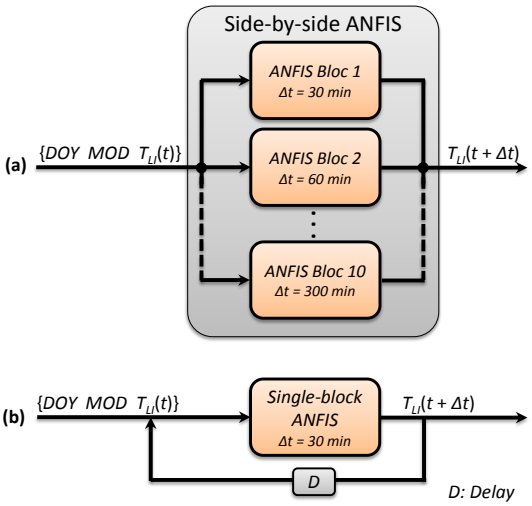

Fig. 3. The two ANFIS forecasting approaches

The first model (Fig. 3.a), is composed of ten different blocks, each one giving a forecast at a specific time horizon (varying from 30 minutes to 5 hours). To obtain the forecasted turbidity ($T_{LI}(t + \Delta t)$), the inputs considered for each block are: the day of the year DOY, the minutes of the day MOD) and the atmospheric turbidity $T_{LI}(t)$.

The second model (Fig. 3.b), consists of a single block giving forecasts at a multiple of 30 minutes. The output of the block is re-injected into the input until the desired time horizon is reached. A criterion has been considered for evaluating the performance of the models: the Normalized Root-Mean-Square Error (NRMSE).

5. RESULTS

This section is organized as follows: first, we present the constraints upon the model regarding to clear sky DNI forecasting. Then the optimization of the ANFIS models is described. Finally, we compare the optimized models we propose with the standard models presented in the previous section of the paper.

5.1 Forecasting issues

The main drawback of the clear sky DNI forecasting remains the discontinuity of data due to nights and cloud events. As mentioned above, we only save the full clear sky days in order to keep the transient behavior of the atmospheric turbidity through the day. However, such days are rarely one after the other. It prevents models to get information from previous days and so, only the information of the current clear sky dat is available. It strongly limits the potential of our forecasting model. Indeed, the first turbidity value is obtained after sunrise and so the first clear sky DNI forecast is available at sunrise plus horizon. For instance, if sunrise occurs at 8:00 AM and the forecast horizon is set to 5 hours, then the first forecasted value will be available at 01:00 PM using a persistent model. This is the main reason why models based on mean values of turbidity (independent of time) are so convenient. The goal of the ANFIS approaches is to quantify the gain in accuracy reached by the forecasting model as soon as intra-day forecasts are available. If this approach is conclusive, a strategy will be implemented in order to fill the gap produced by nights and clouds in the frame of a real-time processing system.

5.2 ANFIS optimization

A parametric study dealing with forecasting accuracy, for both the side-by-side and the single-block ANFIS, has been performed. The goal is to optimize the structure of the neuro-fuzzy systems used in order to get the lowest possible NRMSE along the forecast horizon. Among the possibilities of optimization, the number of previous observations to be considered, the number of fuzzy sets used to split the universes of discourse of the model inputs and the number of training examples have been optimized. Results are reported below.

Side-by-side ANFIS. Because of the structure of the model, it is not relevant to consider more than one previous observation. Indeed, it has been seen before that forecasted values are not available while the fixed horizon is not elapsed. Two previous observations to be considered and a 5-hour forecast horizon would lead to forecasted values available 10 hours after the sunrise time, which is not realistic. In addition, the way the universes of discourse are partitioned into fuzzy sets is optimized. The side-by-side ANFIS are composed of 3 inputs each and Gaussian membership functions are associated to the sets. It has been decided to consider 2, 3 and 4 fuzzy sets for each block input, what leads to 27 possible configurations. Fig. 4 shows the NRMSE we obtained for each configuration and a forecast horizon varying from 1 to 5 hours. From this graph, it can be noticed easily that only the number of fuzzy sets used to split the universe of discourse of the first input (DOY, the Day Of the Year) impacts accuracy in a significant way. As a consequence, we decided for two fuzzy sets for MOD (the Minute Of the Day) and T_{LI} in order to limit the complexity of the model.

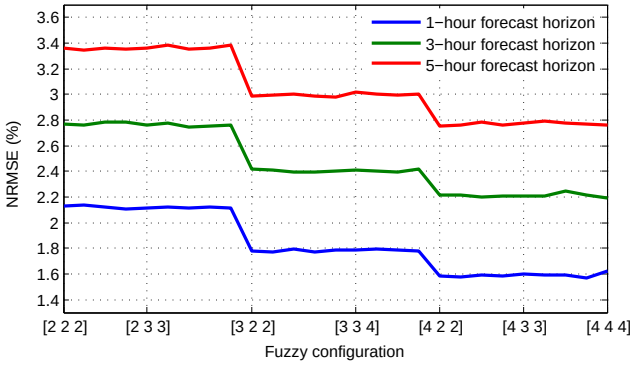

Fig. 4. NRMSE as a function of the number of fuzzy sets used to split the universes of discourse

Regarding to the first model input (DOY), we considered up to 7 fuzzy sets during the parametric analysis we carried out. Results are reported in table 2. Due to the similar evolution of NRMSE for each ANFIS block, only the block dealing with a 5-hour forecast horizon is presented here. As a key result, we found that 5 fuzzy sets is the most suitable regarding to accuracy (about 3 % for a 5-hour forecast horizon). The benefits of a higher number of fuzzy sets are insignifiant but compexity increases. As a result, final configuration is [5 2 2].

Table 2. Fuzzy partition of DOY

Forecast horizon = 5h ; Configuration = [X 2 2]						
X	2	3	4	5	6	7
NRMSE (%)	3.36	3.18	3.11	3.06	3.02	2.99

Once the optimal partition is found, one can search for the optimal number of examples to be used during training. Fig. 5 deals with the NRMSE as a function of the number of training examples, on the basis of fuzzy configuration [5 2 2] and for forecast horizons of 1, 3 and 5 hours. Finally, we decided for 10000 examples as the optimal number of examples to be used during training. Additional examples do not bring more usable information and, as a result, accuracy is not improved significantly.

Single-block ANFIS. A similar optimization process has been performed for the single-block approach. Because of the structure of the ANFIS, the way observations impact on accuracy can be considered. As previously highlighted, the output of the model is used as an input at the next time step, until the desired forecast horizon is reached. Using this structure, the first forecasted value is obtained at the same time than with the side-by-side ANFIS approach, considering only one observation ($T_{LI}(t)$), and 30 minutes

later when using two observations ($T_{LI}(t)$ and $T_{LI}(t-30$ min)). However, the constraints on our database (i.e. discontinuities) as well as some divergence effects limit the number of previous values one can consider to 3 (up to $T_{LI}(t-60$ min)). Table 3 deals with the NRMSE as a function of the number of observations and the number of training examples, with fuzzy configuration [2 2 2].

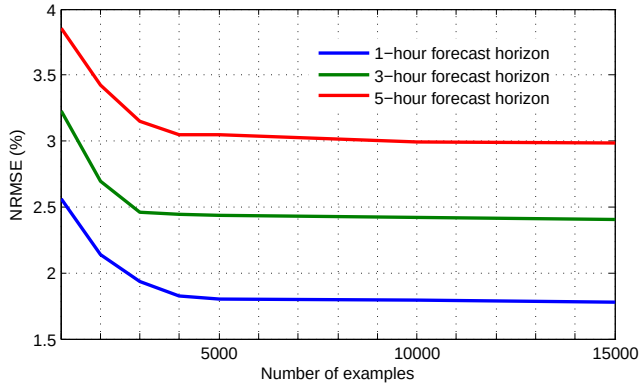

Fig. 5. NRMSE as a function of the number of examples used during training

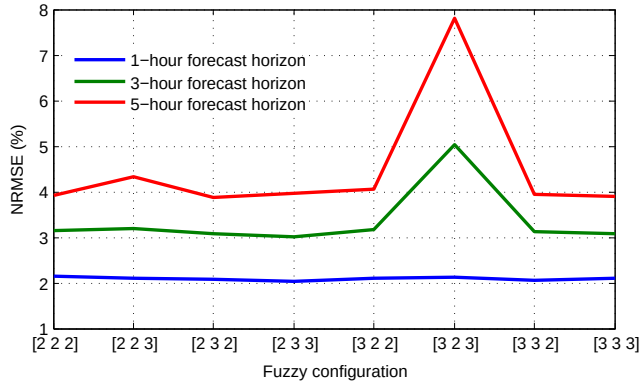

Fig. 6. NRMSE as a function of the fuzzy configuration (model inputs)

Table 3. NRMSE as a function of the number of observations and training examples

Horizon	1 hour			3 hours			5 hours		
Observ.	1	2	3	1	2	3	1	2	3
10000	2.12	1.98	2.29	3.04	3.12	X	3.76	3.94	X
20000	2.12	1.95	2.33	3.08	3.02	X	3.79	3.90	X
30000	2.13	1.96	1.93	3.02	3.04	X	3.78	3.94	X
40000	2.10	1.95	1.95	3.05	3.00	X	3.74	3.84	X
50000	2.11	1.95	1.93	3.07	3.02	X	3.80	3.94	X
60000	2.13	1.95	1.94	3.04	3.07	X	3.76	3.90	X

X: divergence

Taking a look at the results, one can note that an increase in the number of observations do not improve accuracy in a significant way. For a forecast horizon set to 1 hour, accuracy is better when considering 2 observations ($T_{LI}(t)$ and $T_{LI}(t-30$ min)) than only one. For longer forecast horizons, accuracy is the best with only one observation ($T_{LI}(t)$) used as a model input. As a result, we decided for only one observation when the forecast horizon is set to 5 hours. Regarding the number of examples to be used during training, its impact on accuracy is insignificant beyond 10000. So, we used 10000 examples to train the system and optimize its parameters. Finally, as we did for the side-by-side ANFIS, we optimized the partition of the (inputs) universes of discourse. Taking a look at Fig. 6, one can see that, in most cases, the fuzzy configuration does not influence accuracy. As a result, we decided for fuzzy configuration [2 2 2] in order to reduce as possible the complexity of the model and the number of fuzzy rules.

5.3 Forecasting results and discussion

In this section, we compare the results we obtained using the two neuro-fuzzy approaches with the results given by the persistent models or the models based on the calculation of mean values of turbidity. Fig. 7 and 8 summarize these results. The persistent model only based on irradiance is not plotted here because error is to high to be displayed: $NRMSE_{p1} = 31\,\%$ at $t+5$ hours.

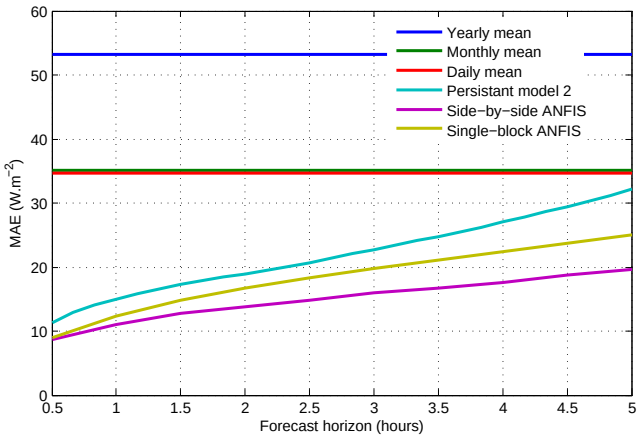

Fig. 7. MAE as a function of the forecast horizon

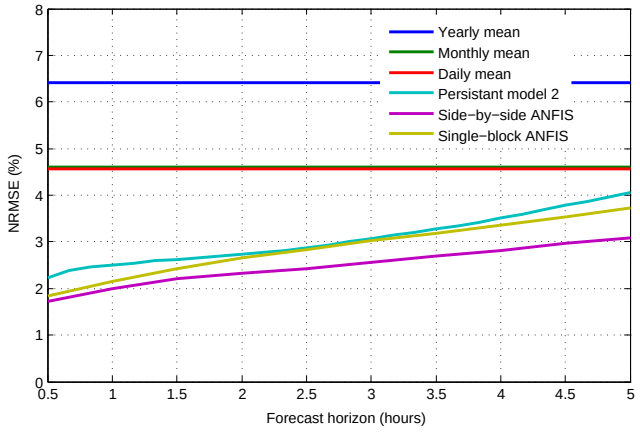

Fig. 8. NRMSE as a function of the forecast horizon

As expected, the benefits in considering the atmospheric turbidity is obvious: accuracy is increased of about 30 % for a 5-hour forecast horizon. One can highlight the stability of the turbidity coefficient in comparison to the variability of sun irradiance through the day. Regarding to the mean turbidity coefficient, the MAE and NRMSE are not related to the forecast horizon and we find that the monthly mean turbidity significantly outperformed the yearly one (18 % of difference in NRMSE). This is due to the seasonal trend depicted earlier. However, the daily mean turbidity does not achieve much better results than

the monthly one (less than 0.5 % of difference). It means that there is no real benefits in interpolating turbidity below the month scale. In other words, the intra-month variability of turbidity is more influenced by the day-by-day atmospheric phenomena than by the overall evolution of the atmosphere through the year. Finally, the persistent model based on atmospheric turbidity outperforms the models using mean turbidity values even if at $t + 5$ hours the MAE and NRMSE are close (difference is 0.6 %).

Whatever the error criterion (MAE or NRMSE), the side-by-side ANFIS give the best forecasting results. The single-block ANFIS is almost equivalent to the side-by-side ANFIS if we consider the MAE only: 20 W/m^2 (side-by-side ANFIS) vs. 24 W/m^2 (single-block ANFIS) at $t + 5$ hours. However, it gives similar results as the Persistent Model 2 (PM2) when considering the NRMSE: 4.05 % (PM2) vs. 3.72 % (single-block ANFIS) at $t + 5$ hours. It means that the single-block ANFIS produces clear sky DNI forecasting with a higher accuracy than the persistent model (MAE is lower) but with more outliers values than the side-by-side ANFIS (NRMSE is higher). To conclude, among the seven modelling approaches we tested, the side-by-side ANFIS model appears to forecast the clear sky DNI with unsurpassed accuracy ($NRMSE = 3\,\%$).

6. CONCLUSION

The error calculated between the measured DNI and the expected ones, using a daily mean value of the turbidity ($NRMSE_{\langle Day \rangle} = 4.5\,\%$), encouraged us to develop intra-day forecasting models of the clear sky irradiance. As a consequence, two different approaches based on Adaptive Network-based Fuzzy Inference Systems (ANFIS) have been developed in this paper in order to forecast clear sky DNI for a horizon varying from 30 minutes to 5 hours. Both approaches outperformed the persistent models. The side-by-side ANFIS provided the best results. However, this model is hard to implement because of its structure. Indeed, an ANFIS block has to be developed and optimized for each forecast horizon. On the other hand, the single-block ANFIS has the huge advantage to be less complex, easier to optimize and more easily adaptable to different time scales. Nevertheless, it produces slightly less accurate estimates than the side-by-side ANFIS, even if results remain better than those produced by the persistent models.

REFERENCES

Ajith Abraham. Adaptation of fuzzy inference system using neural learning. In Nadia Nedjah and Luiza de Mourelle, editors, *Fuzzy system engineering*, volume 181 of *Studies in Fuzziness and Soft Computing*, pages 53–83. Springer Berlin Heidelberg, 2005.

International Energy Agency. *Technology Roadmap: Concentrating Solar Power*. OECD Publishing, May 2010.

A. Cazorla, F.J. Olmo, and L. Alados-Arboledas. Development of a sky imager for cloud cover assessment. *Journal of the Optical Society of America A*, 25(1):29–39, 2008.

Chin Wai Chow, Bry Urquhart, Matthew Lave, Anthony Dominguez, Jan Kleissl, Janet Shields, and Byron Washom. Intra-hour forecasting with a total sky imager at the UC san diego solar energy testbed. *Solar Energy*, 85(11):2881–2893, 2011.

Ingrid Daubechies. *Ten lectures on wavelets*, volume 61 of *CBMS-NSF Regional Conference Series in Applied Mathematics*. Society for Industrial and Applied Mathematics, 1992.

Maimouna Diagne, Mathieu David, Philippe Lauret, John Boland, and Nicolas Schmutz. Review of solar irradiance forecasting methods and a proposition for small-scale insular grids. *Renewable and Sustainable Energy Reviews*, 27:65–76, 2013. ISSN 1364-0321.

J.C. Grenier, A. De La Casinière, and T. Cabot. A spectral model of Linke's turbidity factor and its experimental implications. *Solar Energy*, 52(4):303–313, 1994.

Christian A. Gueymard. REST2: High-performance solar radiation model for cloudless-sky irradiance, illuminance, and photosynthetically active radiation – validation with a benchmark dataset. *Solar Energy*, 82(3): 272–285, 2008.

Christian A. Gueymard. Clear-sky irradiance predictions for solar resource mapping and large-scale applications: Improved validation methodology and detailed performance analysis of 18 broadband radiative models. *Solar Energy*, 86(8):2145–2169, 2012a. ISSN 0038-092X.

Christian A. Gueymard. Temporal variability in direct and global irradiance at various time scales as affected by aerosols. *Solar Energy*, 86:3544–3553, 2012b.

Christian A. Gueymard and Daryl R. Myers. Validation and ranking methodologies for solar radiation models. In Viorel Badescu, editor, *Modeling Solar Radiation at the Earth's Surface*, pages 479–510. Springer Berlin Heidelberg, 2008.

Pierre Ineichen and Richard Perez. A new airmass independent formulation for the linke turbidity coefficient. *Solar Energy*, 73(3):151–157, 2002. ISSN 0038-092X. doi: http://dx.doi.org/10.1016/S0038-092X(02)00045-2.

Fritz Kasten. Elimination of the virtual diurnal variation of the Linke turbidity factor. *Meteorologische Rundschau*, 41(3):93–94, 1988.

Fritz Kasten and Andrew T. Young. Revised optical air mass tables and approximation formula. *Applied Optics*, 28(22):4735–4738, 1989.

Chin-Teng Lin and C.S. Goerges Lee. *Neural Fuzzy Systems: A Neuro-Fuzzy Synergism to Intelligent Systems*. Prentice-Hall, Upper Saddle River, NJ, 1996.

F Linke. Transmisions-koeffizient und trübungsfaktor. *Beitr. Physik. fr. Atmos.*, 10:91–103, 1922.

Ricardo Marquez and Carlos F M Coimbra. Intra-hour DNI forecasting based on cloud tracking image analysis. *Solar Energy*, 91:327–336, 2013. ISSN 0038-092X.

A Mefti, A Adane, and M Y Bouroubi. Satellite approach based on cloud cover classification: Estimation of hourly global solar radiation from meteosat images. *Energy Conversion and Management*, 49:652–659, 2008.

Julien Nou, Rémi Chauvin, Adama Traoré, Stéphane Thil, and Stéphane Grieu. Atmospheric turbidity forecasting using side-by-side ANFIS. In *SolarPACES*, 2013.

Ali Zaher. *Traitement d'images METEOSAT: Prediction de l'irradiation solaire et controle supervise de capteurs solaires*. PhD thesis, University of Perpignan, PROMES laboratory, 2012.